Dioxododecenoic Acid: A Lipid Hydroperoxide-Derived Bifunctional Electrophile Responsible for Etheno DNA Adduct Formation

ARTICLE *in* CHEMICAL RESEARCH IN TOXICOLOGY · APRIL 2005

Impact Factor: 3.53 · DOI: 10.1021/tx049716o · Source: PubMed

4 AUTHORS, INCLUDING:

Seon Hwa Lee
Tohoku University
76 PUBLICATIONS **2,465** CITATIONS
SEE PROFILE

Maria Victoria Silva Elipe
Amgen
34 PUBLICATIONS **1,257** CITATIONS
SEE PROFILE

Ian A Blair
University of Pennsylvania
428 PUBLICATIONS **12,435** CITATIONS
SEE PROFILE

Dioxododecenoic Acid: A Lipid Hydroperoxide-Derived Bifunctional Electrophile Responsible for Etheno DNA Adduct Formation

Seon Hwa Lee, Maria V. Silva Elipe,† Jasbir S. Arora, and Ian A. Blair*

Center for Cancer Pharmacology, University of Pennsylvania School of Medicine, Philadelphia, Pennsylvania 19104-6160

Received October 12, 2004

It has been proposed that 13(*S*)-hydroperoxy-9*Z*,11*E*-octadecadienoic acid [13(*S*)-HPODE]-mediated formation of 4-oxo-2(*E*)-nonenal and 4-hydroxy-2(*E*)-nonenal arises from a Hock rearrangement. This suggested that a 4-oxo-2(*E*)-nonenal-related molecule, 9,12-dioxo-10(*E*)-dodecenoic acid (DODE), could also result from the intermediate formation of 9-hydroperoxy-12-oxo-10(*E*)-dodecenoic acid. A recent report has described the formation of DODE-derived etheno adducts when 13(*S*)-HPODE was allowed to decompose in the presence of 2′-deoxynucleosides or DNA. However, the regioselectivity of lipid hydroperoxide-derived DODE addition to 2′-deoxyguanosine (dGuo) or other 2′-deoxynucleosides was not determined. The structure of carboxynonanone-etheno-dGuo formed from vitamin C-mediated 13(*S*)-HPODE decomposition has now been established by a combination of ^{1}H and ^{13}C NMR spectroscopy studies of its bis-methylated derivative. The site of dGuo methylation was first established as being at *N*-5 rather than at *O*-9 from NMR analysis of a methyl derivative of the model compound, heptanone-etheno-dGuo. ^{1}H,^{13}C 2D heteronuclear multiple bond correlations were then used to establish unequivocally that the bis-methyl derivative of carboxynonanone-etheno-dGuo was 3-(2′-deoxy-β-D-erythropentafuranosyl)imidazo-7-(9″-carboxymethylnona-2″-one)-9-oxo-5-*N*-methyl[1,2-*a*]purine rather than its 6-(9″-carboxymethylnona-2”-one)-9-oxo-5-*N*-methyl-[1,2-*a*]purine regioisomer. Therefore, etheno adduct formation occurred by initial nucleophilic attack of the exocyclic N^2 amino group of dGuo at the C-12 aldehyde of DODE to form an unstable carbinolamine intermediate. This was followed by intramolecular Michael addition of the pyrimidine *N*1 of dGuo to C-11 of the resulting α,β-unsaturated ketone. Subsequent dehydration gave 3-(2′-deoxy-β-D-erythropentafuranosyl)imidazo-7-(9″-carboxynona-2″-one)-9-oxo-[1,2-*a*]purine (carboxynonanone-etheno-dGuo). An efficient synthesis of DODE was developed starting from readily available 1,8-octanediol using a furan homologation procedure. This synthetic method allowed multigram quantities of DODE to be readily prepared. Synthetic DODE when reacted with dGuo gave carboxynonanone-etheno-dGuo that was identical with that derived from vitamin C-mediated 13(*S*)-HPODE decomposition in the presence of dGuo.

Introduction

Oxidation of ω-6 polyunsaturated fatty acids (PUFAs)[1] during oxidative stress occurs through both enzymatic and nonenzymatic pathways (*1*−*3*). The resulting ω-6 PUFA-derived lipid hydroperoxides such as 13-hydroperoxy-9*Z*,11*E*-octadecadienoic acid (13-HPODE) can then undergo Fe^{II}-, Cu^{I}-, or vitamin C-mediated homolytic decomposition to form α,β-unsaturated aldehydes through two distinct pathways (Scheme 1) (*4*−*6*). The first pathway, which most likely involves α-cleavage of an alkoxy radical, results in the formation of 4,5-epoxy-2(*E*)-decenal (EDE) (*6*). The second pathway involves the formation of 4-hydroperoxy-2(*E*)-nonenal (HPNE), which undergoes dehydration to 4-oxo-2(*E*)-nonenal (ONE) or reduction to 4-hydroxy-2(*E*)-nonenal (HNE) (*6*, *7*). The α,β-unsaturated aldehydes act as bifunctional electrophiles that can covalently modify nucleosides, DNA, amino acids, and proteins (*8*−*12*). ONE reacts with 2′-deoxyguanosine (dGuo), 2′-deoxyadenosine (dAdo), and 2′-deoxycytidine (dCyd) in DNA or as the free nucleosides to form 3-(2′-deoxy-β-D-erythropentafuranosyl)imidazo-7-(heptane-2″-one)-9-oxo-[1,2-*a*]purine (heptanone-etheno-dGuo) (*13*), heptanone-etheno-dAdo (*14*, *15*), and heptanone-etheno-dCyd (*16*), respectively (Scheme 2). ONE also reacts with free arginine to form an imidazole adduct (*17*) and with lysine and histidine to form novel cyclic pyrrole adducts

* To whom correspondence should be addressed. Fax: 215-573-9889. E-mail: ian@spirit.gcrc.upenn.edu.

† Present address: Amgen, Analytical Sciences Department, One Amgen Center Drive, Thousand Oaks, CA 91320.

[1] Abbreviations: APCI, atmospheric pressure chemical ionization; bd, broad doublet; bs, broad singlet; bt, broad triplet; CID, collision-induced dissociation; COSY, ^{1}H−^{1}H 2D correlation spectroscopy; COX, cyclooxygenase; dAdo, 2′-deoxyadenosine; d, doublet; dd, doublet of doublets; ddd, doublet of doublet of doublets; dCyd, 2′-deoxycytidine; dGuo, 2′-deoxyguanosine; DEAD, diethyl azodicarboxylate; DODE, 9,-12-dioxo-10(*E*)-dodecenoic acid; dt, double triplet; etheno-dGuo, 1,N^2-etheno-dGuo; heptanone-etheno-dGuo, 3-(2′-deoxy-β-D-erythropentafuranosyl)imidazo-7-(heptane-2″-one)-9-oxo-[1,2-*a*]purine; EDE, 4,5-epoxy-2(*E*)-decenal; GSH, glutathione; HMBC, ^{1}H,^{13}C 2D heteronuclear multiple bond correlation; HNE, 4-hydroxy-2(*E*)-nonenal; HODD, 9-hydroxy-12-oxo-10(*E*)-dodecenoic acid; 15(*S*)-HPETE, 15(*S*)-hydroperoxy-5*Z*,8*Z*,11*Z*,13*E*-eicosatetraenoic acid; HPNE, 4-hydroperoxy-2(*E*)-nonenal; HPODD, 9-hydroperoxy-12-oxo-10(*E*)-dodecenoic acid; 13(*S*)-HPODE, 13(*S*)-hydroperoxy-9*Z*,11*E*-octadecadienoic acid; HSQC, ^{1}H,^{13}C 2D heteronuclear single quantum correlation; m, multiplet; MH^{+}, protonated molecular ion; MS^{n}, multiple tandem mass spectrometry; MOPS, morpholinopropanesulfonic acid; NA, not available; ONE, 4-oxo-2(*E*)-nonenal; PDC, pyridinium dichromate; PUFA, polyunsaturated fatty acid; quint, quintet; ROESY, rotating-frame Overhauser enhancement spectroscopy; s, singlet; SPE, solid phase extraction; t, triplet; TBDMS, *tert*-butyldimethylsilyl.

10.1021/tx049716o CCC: $30.25
Published on Web 02/18/2005

Scheme 1. Formation of Bifunctional Electrophiles from Lipid Peroxidation

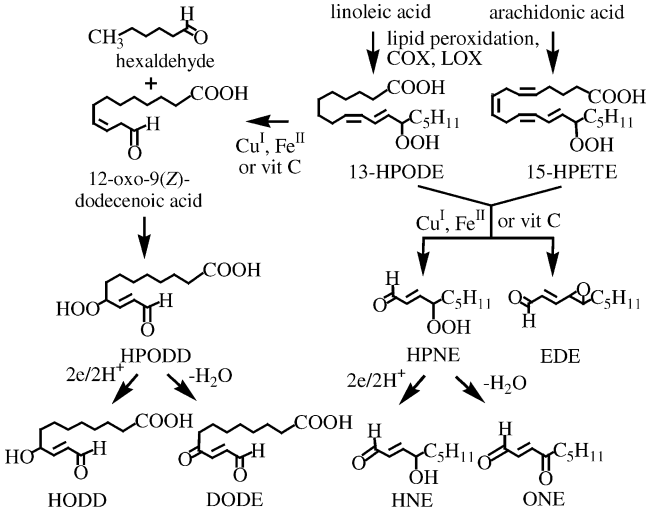

Scheme 2. Formation of DNA Adducts from Lipid Peroxidation

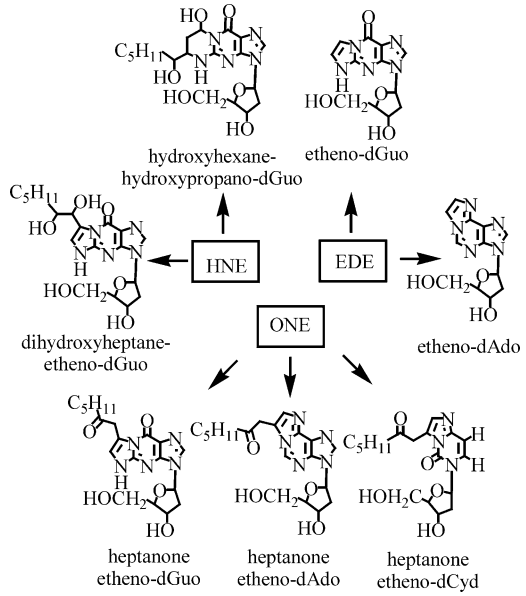

(*18*−*20*). EDE can interact with dGuo or dAdo in DNA or as the free nucleosides to give unsubstituted 1,N^2-etheno-dGuo (etheno-dGuo) and etheno-dAdo, respectively (Scheme 2) (*21*). Etheno-dGuo is mutagenic in mammalian cells (AA8 CHO), inducing base pair mutations, with a preference for G to A transitions (*22*). Etheno-dAdo is more mutagenic in human cells (HeLa) than 8-oxo-dGuo, inducing A to T transversions in experiments using modified double- and single-stranded DNA substrates (*23*). HNE can form hydroxypropano-dGuo adducts although it has a low reaction rate with nucleobases (Scheme 2). Only one hydroxypropano-dGuo adduct/10^6 normal bases was detected in cells cultured with 20 mM HNE for 24 h (*24*). Despite this low reactivity, hydroxypropano-dGuo adducts have been identified in mammalian tissue DNA (Scheme 2) (*25*). In contrast, when HNE is oxidized in vitro by lipid hydroperoxides, a more efficient reaction occurs through the formation of 2,3-epoxy-4-hydroxy-nonanal. The regioselectivity of reaction with dGuo is modified so that dihydroxyheptane-etheno adducts are formed (*26*). However, it has been suggested that a reaction between HNE and lipid hydroperoxides is unlikely to occur in cells because of the relatively high pK_a of the latter compounds (*25*). HNE appears to be much more reactive toward amino acids and proteins than it is with DNA bases. It covalently modifies cysteine, histidine, and lysine residues to give THF adducts through Michael addition (*12*) and with lysine and histidine residues to give pyrrole adducts through Schiff base formation (*12*, *27*−*29*).

It has been proposed that 13-HPODE-mediated formation of ONE and HNE requires a Hock rearrangement through the intermediate formation of a bis-hydroperoxide intermediate, which arises from oxygenation at C-10 (*7*, *12*). However, a direct Hock rearrangement of 13-HPODE would lead to the intermediate formation of 12-oxo-9(*Z*)-dodecenoic acid (*12*), a carboxylate analogue of 3(*Z*)-nonenal (*30*). 3(*Z*)-Nonenal is known to rapidly form HPNE (*30*), which in turn is converted to ONE and HNE (*6*, *7*). Therefore, the ONE-related molecule, 9,12-dioxo-10(*E*)-dodecenoic acid (DODE), could also be formed from 13-HPODE through the intermediate formation of 12-oxo-9(*Z*)-dodecenoic acid and 9-hydroperoxy-12-oxo-10(*E*)-dodecenoic acid (HPODD) (Scheme 1). This raised the possibility that a novel bifunctional electrophile could result from linoleic acid peroxidation, which could modify DNA and proteins in a manner similar to ONE. DODE as its 10(*Z*)-isomer was detected as a linoleic acid peroxidation product from lentil seeds, and its structure was confirmed by total synthesis (*31*). It was presumed to arise through intermediate formation of 9-HPODE. Reactions of 13(*S*)-hydroperoxy-9*Z*,11*E*-octadecadienoic acid [13(*S*)-HPODE] with enzyme preparations of both soybean and alfalfa seedlings resulted in the formation of 9-hydroxy-12-oxo-10(*E*)-dodecenoic acid (HODD) (*32*, *33*). The formation of HODD implies that there was an intermediate formation of HPODD. The reduction of HPODD in a manner similar to HPNE (6) would lead to the formation of HODD, whereas dehydration would lead to DODE (Scheme 1). Further evidence for the intermediate formation of HPODD comes from the detection of HODD in trace amounts during the autoxidation of linoleic acid (*34*, *35*). A recent report has described the formation of DODE-derived etheno adducts when 13-HPODE was allowed to decompose in the presence of 2′-deoxynucleosides or DNA (*36*). The present study was undertaken to establish the regioselectivity of DODE-mediated etheno adduct formation and to develop a convenient route for its preparation. This will then permit a thorough evaluation of its biochemical properties and its reaction with nucleosides, amino acids, and proteins.

Materials and Methods

Materials. Ammonium acetate, ascorbic acid, dGuo, diethyl ether, diisopropylethylamine (DIPE), iodomethane-^{13}C, sodium chloride, sodium sulfate, soybean lipoxidase, and other chemicals were purchased from Sigma-Aldrich. (St. Louis, MO). Linoleic acid and arachidonic acid were purchased from Cayman Chemical Co. (Ann Arbor, MI). 3-Morpholinopropanesulfonic acid (MOPS) was obtained from Fluka BioChemika (Milwaukee, WI). Supelclean LC-18 solid phase extraction (SPE) columns were from Supelco (Bellefonte, PA). Chelex-100 chelating ion exchange resin (100−200 mesh size) was purchased from Bio-Red Laboratories (Hercules, CA). HPLC grade water, acetonitrile, and methanol were obtained from Fisher Scientific Co. (Fair Lawn, NJ). ACS grade ethanol was obtained from Pharmco (Brookfield, CT). Gases were supplied by BOC Gases (Lebanon, NJ).

Liquid Chromatography. Chromatography for LC/MS experiments was performed using a Waters Alliance 2690 HPLC system (Waters Corp., Milford, MA). Purification of dGuo adducts was conducted on a Hitachi L-6200 Intelligent Pump (Hitachi, San Jose, CA) equipped with a Hitachi L-4000 UV detector. Gradient elution was performed in the linear mode. Gradient system 1 included a Hi-Chrom silica column (250 mm × 4.6 mm i.d., 5 μm; Regis, Morton Grove, IL) at a flow rate of 1 mL/min. An YMC C_{18} ODS-AQ column (250 mm × 4.6 mm i.d., 5 μm; Waters) was used in systems 2−4 with a flow rate of 1.0 mL/min. For system 1, solvent A was hexane and 2-propanol (197:3, v/v) and solvent B was hexane and 2-propanol (7:3, v/v). The gradient conditions were as follows: 3% B at 0 min, 3% B at 15 min, 85% B at 28 min, and 3% B at 30 min. For system 2, solvent A was THF, methanol, water, and acetic acid (25:30:44.9:0.1, v/v) and solvent B was methanol and water (9:1, v/v). Both solvents A and B contained 5 mM ammonium acetate. The gradient conditions were as follows: 70% B at 0 min, 70% B at 3 min, 100% B at 10 min, 100% B at 20 min, and 70% B at 23 min, followed by a 7 min equilibration time. For system 3, solvent A was 5 mM ammonium acetate in water and solvent B was 5 mM ammonium acetate in acetonitrile. The linear gradient was as follows: 6% B at 0 min, 6% B at 3 min, 20% B at 9 min, 20% B at 13 min, 60% B at 21 min, 80% B at 22 min, and 80% B at 24 min. For system 4, solvent A was water and solvent B was acetonitrile. The linear gradient for system 4 was as follows: 20% B at 0 min, 20% B at 3 min, 45% B at 17 min, 80% B at 19 min, and 80% B at 26 min. All separations except for system 1 were performed at ambient temperature.

Mass Spectrometry. Mass spectrometry was conducted with a Thermo Finnigan LCQ ion trap mass spectrometer (Thermo Finnigan, San Jose, CA) equipped with an atmospheric pressure chemical ionization (APCI) source in the positive ion mode. The LCQ operating conditions were as follows: vaporizer temperature at 450 °C, heated capillary temperature at 150 °C, with a discharge current of 5 μA applied to the corona needle. Nitrogen was used as the sheath (80 psi) and auxiliary (10 arbitrary units) gas to assist with nebulization. Full scanning analyses were performed in the range of *m/z* 100−800. Collision-induced dissociation (CID) experiments coupled with multiple tandem mass spectrometry (MS^n) employed helium as the collision gas. The relative collision energy was set at 20% of the maximum (1 V).

NMR. The NMR spectra were determined at 25 °C on a Varian Inova 600 MHz instrument equipped with a Nalorac 3 mm indirect detection gradient probe. ^{13}C experiments were performed at 150 MHz. The samples (ca. 0.5 mg for methylated heptanone-etheno-dGuo, methylated carboxynonanone-etheno-dGuo, and carboxynonanone-etheno-dGuo and ca. 0.2 mg for ^{13}C-methylated heptanone-etheno-dGuo) were dissolved in 150 μL of DMSO-d_6. The data processing was conducted on the spectrometer. Chemical shifts are reported in the δ scale (ppm) by assigning the residual solvent peak to 2.49 and 39.5 ppm for DMSO for ^1H and ^{13}C, respectively. The rotating-frame nuclear Overhauser effect (ROESY) experiment was determined with a 300 ms mixing time. The delay between successive pulses was 1 s for $^1H-^1H$ 2D correlation spectroscopy (COSY) and ROESY. Both the ^1H,^{13}C 2D heteronuclear single quantum correlation (HSQC) and the ^1H,^{13}C 2D heteronuclear multiple bond correlation (HMBC) spectra were determined using gradient pulses for coherence selection. The HSQC spectrum was determined with decoupling during acquisition. Delays corresponding to one bond $^{13}C-^1H$ coupling (ca. 140 Hz) for the low-pass filter and to two-to-three bond $^{13}C-^1H$ long-range coupling (5, 7, or 10 Hz) were used for the HMBC.

Preparation of 13(*S*)-HPODE. 13(*S*)-HPODE was prepared using linoleic acid and soybean lipoxidase in 0.2 M Chelex-treated borate buffer (pH 9.0) as described previously (*37*).

Preparation of 15(*S*)-Hydroperoxy-5*Z*,8*Z*,11*Z*,13*E*-eicosatetraenoic Acid [15(*S*)-HPETE]. 15(*S*)-HPETE was prepared using arachidonic acid (25 mg, 82.2 μmol) and soybean lipoxidase (type V, 1 mg) in 30 mL of 0.2 M Chelex-treated borate buffer (pH 9.0). The reaction was performed at 0 °C under oxygen with constant stirring. After 5 h, the reaction mixture was acidified to pH 3 with 1 N HCl and the 15(*S*)-HPETE was extracted with diethyl ether (2 × 5 mL). The combined extracts were washed with water, dried over sodium sulfate, and evaporated under a stream of nitrogen. The 15(*S*)-HPETE was then purified using normal phase gradient system 1 (retention time, 11.4 min). The pure 15(*S*)-HPETE was dissolved in ethanol, and its concentration was determined by UV spectroscopy (λ_{max} 236 nm, $\epsilon = 27\,000$). It was stored in ethanol at −70 °C, and the solution was reanalyzed by reversed phase LC/MS using gradient system 2 before it was used. A single chromatographic peak was observed at a retention time of 9.5 min. The mass spectrum contained a dominant ammoniated molecular ion at *m/z* 354 $[M + NH_4]^+$ together with the expected fragment ion at *m/z* 219 $[M - C_6H_{12}OOH]^+$. When the pure 15(*S*)-HPETE was analyzed by LC/MS/UV under normal phase conditions using system 1, no early eluting peaks corresponding to α,β-unsaturated aldehydes were detected. The 15(*S*)-HPETE was shown to contain <1% of the 15(*R*)-enantiomer by reduction with triphenylphosphine to 15-hydroxy-5*Z*,8*Z*,11*Z*,13*E*-eicosatetraenoic acid, formation of a pentafluorobenzyl ester derivative, and analysis by chiral LC/electron capture APCI/MS. Chromatography was conducted using 2-propanol/methanol/hexane as the mobile phase with a Chiralpak AD-H column (250 mm × 4.6 mm i.d., 5 μm; Daicel Chemical Industries, Ltd., Tokyo, Japan) at a flow rate of 1 mL/min as described previously (*38*).

8-(1,1,2,2-Tetramethyl-1-silapropoxy)octan-1-ol (1). Sodium hydride dispersion in mineral oil (900 mg, 37.5 mmol) was washed with hexanes and then suspended in THF (250 mL). 1,8-Octanediol (5 g, 34.2 mmol) was added to the suspension, and the reaction mixture was stirred for 20 h under argon. *tert*-Butyldimethylsilyl (TBDMS) chloride (5.2 g, 34.5 mmol) was then added, and stirring was continued for a further 4 h. After filtration, the solvent was evaporated under reduced pressure. The crude product was purified on a silica gel column using 15% ethyl acetate in hexanes to afford the monosilyl ether (**1**; 6.1 g, 69%). The ^1H NMR spectrum (500 MHz, $CDCl_3$, δ) was similar to that reported previously (*39*): 0.04 [s, 6H, $Si(CH_3)_2$], 0.88 [s, 9H, $SiC(CH_3)_3$], 1.30−1.34 (m, 8H, CH_2 from C-3, C-4, C-5, C-6), 1.50 (quint, $J = 6.6$ Hz, 2H, CH_2 from C-2), 1.55 (quint, $J = 6.6$ Hz, 2H, CH_2 from C-7), 3.59 (t, $J = 6.5$ Hz, 2H, CH_2 from C-1), 3.62 (t, $J = 6.5$ Hz, 2H, CH_2 from C-8).

8-Bromo-1-(1,1,2,2-tetramethyl-1-silapropoxy)octane (2). Zinc bromide (5.494 g, 24.4 mmol) in THF (100 mL) was added to a magnetically stirred solution of **1** (6.1 g, 24.4 mmol) and triphenylphosphine (19.2 g, 73.2 mmol) in THF (300 mL) under argon. After the solution was stirred for 10 min, diethyl azodicarboxylate (DEAD, 15.37 mL, 97.6 mmol) was added dropwise at 0 °C with a syringe. The reaction mixture was allowed to warm to room temperature, stirred for an additional 1 h, and filtered, and the solvent was evaporated under reduced pressure. The crude product was purified by chromatography on a silica gel column with 1.5% ethyl acetate in hexanes to afford the bromide (**2**; 6 g, 82%). The ^1H NMR spectrum (500 MHz, $CDCl_3$, δ) was similar to that reported previously (*39*): 0.04 [s, 6H, $Si(CH_3)_2$], 0.89 [s, 9H, $SiC(CH_3)_3$], 1.30−1.50 (m, 8H, CH_2 from C-3, C-4, C-5, C-6), 1.66 (quint, $J = 7$ Hz, 2H, CH_2 from C-7), 1.85 (quint, $J = 7$ Hz, 2H, CH_2 from C-2), 3.40 (t, $J = 7$ Hz, 2H, CH_2 from C-8), 3.59 (dt, $J = 7$, 2 Hz, 2H, CH_2 from C-1).

8-(2-Furyl)octan-1-ol (3). *n*-Butyllithium (23 mL, 2.5 M in hexane, 57.5 mmol) was added to furan (6.97 mL, 95.84 mmol) in dried THF (75 mL) under argon at 0 °C. The resulting brown solution was brought to room temperature and stirred for an additional 3 h. Compound **2** (6 g, 19.16 mmol) was added at 0 °C. The reaction mixture was stirred for an additional 4 h and quenched by adding saturated NH_4Cl solution. It was extracted with ethyl acetate, dried (sodium sulfate), and evaporated under reduced pressure. Without further purification, THF (50 mL) and Bu_4NF (77 mL, 1 M in THF, 76.67 mmol) were sequentially added to the residue (5.5 g). The reaction mixture was quenched

by adding saturated NH_4Cl solution and extracted using ethyl acetate. The combined organic layers were dried (sodium sulfate) and evaporated under reduced pressure. The crude product was purified by chromatography on a silica gel column with 25% ethyl acetate in hexanes to afford the furyl alcohol (**3**; 3.2 g, 85%). The ^{1}H NMR spectrum (500 MHz, $CDCl_3$, δ) was similar to that published previously (*40*): 1.28−1.34 (m, 8H, CH_2 from C-3, C-4, C-5, C-6), 1.53−1.64 (m, 4H, CH_2 from C-2, C-7), 2.60 (t, J = 7.5 Hz, 2H, CH_2 from C-8), 3.62−3.64 (m, 2H, CH_2 from C-1), 5.96 (d, J = 2 Hz, 1H, CH from C-3′), 6.26 (dd, J = 0.5, 2 Hz, 1H, CH from C-4′), 7.28 (d, J = 0.5 Hz, 1H, CH from C-5′).

8-(2-Furyl)octanoic Acid (4). Pyridinium dichromate (PDC) (36.85 g, 97.9 mmol) was added to a solution of 8-(2-furyl)octan-1-ol (3.2 g, 16.3 mmol) in DMF (45 mL). The resulting mixture was stirred for 18 h and quenched by adding saturated NH_4Cl solution. After extraction with ethyl acetate, the combined organic layers were washed with citric acid solution (pH 3). The residue was purified on silica gel column using 35% ethyl acetate in hexane to give 8-(2-furyl)octanoic acid (**4**; 2.5 g, 73%). The ^{1}H NMR spectrum (500 MHz, $CDCl_3$, δ) was similar to that published previously (*40*): 1.32−1.35 (m, 6H, CH_2 from C-4, C-5, C-6), 1.61−1.64 (m, 4H, CH_2 from C-3, C-7), 2.33−2.37 (m, 2H, CH_2 from C-2), 2.60 (t, J = 7.5 Hz, 2H, CH_2 from C-8), 5.96 (d, J = 2 Hz, 1H from C-3′), 6.26 (dd, J = 0.5, 2 Hz, 1H from C-4′), 7.28 (d, J = 0.5 Hz, 1H from C-5′).

DODE. To a solution of **4** (2.5 g, 11.9 mmol) and pyridine in THF−acetone−H_2O (5:4:1, 60 mL) was added *N*-bromosuccinimide (NBS; 2.54 g, 14.2 mmol) dissolved in THF−acetone−H_2O (5:4:1, 20 mL) at −20 °C (*41*). The solution was stirred for 1 h at −20 °C followed by 6 h at room temperature and then poured into a mixture of ethyl acetate and aqueous $Na_2S_2O_3$. The organic layer was separated, washed with aqueous citric acid solution (pH 3), dried, and evaporated under reduced pressure. The residue was purified on a silica gel column using 45% ethyl acetate in hexane to afford DODE (1.2 g, 44%). ^{1}H NMR (500 MHz, $CDCl_3$, δ): 1.32−1.36 (m, 6H, CH_2 from C-4, C-5, C-6), 1.64 (m, 4H, CH_2 from C-3, C-7), 2.35 (t, J = 7.5 Hz, 2H, CH_2 from C-2), 2.68 (t, J = 7.5 Hz, 2H, CH_2 from C-8), 6.78 (dd, J = 7, 16 Hz, CH from C-11), 6.86 (d, J = 16 Hz, 1H, CH from C-10), 9.78 (d, J = 7 Hz, 1H, CH from C-12). HRMS (*m/z*): $[M + Na]^+$ calculated for $C_{12}H_{18}O_4$·Na, 249.110279; found, 249.110530. On treatment with diazomethane, an intense MH^+ was observed at *m/z* 263.1 ($C_{13}H_{20}O_4$) corresponding to methylation of the terminal carboxylate.

Vitamin C-Mediated Decomposition of 13-HPODE or 15-HPETE in the Presence of dGuo. A solution of 13-HPODE or 15-HPETE (150 nmol) in ethanol (10 μL) and vitamin C (750 nmol) in Chelex-treated 100 mM MOPS containing 150 mM NaCl (pH 7.4, 10 μL) was added to dGuo (750 nmol) in Chelex-treated 100 mM MOPS containing 150 mM NaCl (pH 7.4, 180 μL). The reaction mixture was sonicated for 15 min at room temperature, incubated at 37 °C for 24 h, and then placed on ice. The samples were filtered through a 0.2 μm Costar cartridge prior to analysis of a portion of the sample (20 μL) by LC/MS using gradient system 3.

Methylation of the Reaction Mixture of 13-HPODE and dGuo. After 24 h of incubation at 37 °C, a portion (100 μL) of the reaction mixture was transferred into a glass tube and evaporated to dryness under nitrogen. The residue was redissolved with 100 μL of methanol and treated with 0.5 mL of ethereal diazomethane. The solution was allowed to stand for 1 h at room temperature, evaporated to dryness under nitrogen, and reconstituted in 100 μL of water. The sample was filtered through a 0.2 μm Costar cartridge prior to analysis of a portion of the sample (20 μL) by LC/MS using gradient system 3.

Preparation of Heptanone-etheno-dGuo and Carboxynonanone-etheno-dGuo for UV, NMR, and LC/MS^n Analysis. A solution of 13(*S*)-HPODE (12.1 μmol) in ethanol (200 μL) and vitamin C (60.5 μmol) in Chelex-treated 100 mM MOPS containing 150 mM NaCl (pH 7.4, 100 μL) were added to dGuo (60.5 μmol) in Chelex-treated 100 mM MOPS containing 150 mM NaCl (pH 8.0, 1700 μL). The reaction mixture was sonicated for 15 min at room temperature and incubated at 60 °C for 36 h. It was placed on ice and heptanone-etheno- and carboxynonanone-etheno-dGuo adducts were isolated using gradient system 3, by monitoring the UV absorbance at 230 nm. The fractions, which eluted between 13.0 and 13.6 min (carboxynonanone-etheno-dGuo) and between 20.3 and 20.9 min (heptanone-etheno-dGuo), were collected and concentrated under nitrogen at room temperature. The residues were dissolved in a 0.5 mL mixture of acetonitrile/water (2:8, v/v) and rechromatographed on the same system. The fractions containing pure heptanone-etheno-dGuo and carboxynonanone-etheno-dGuo (as determined by LC/MS) were combined, concentrated under nitrogen with adding CCl_4 as an azeotropic solvent, and dried under vacuum, respectively. The retention times of pure carboxynonanone-etheno- and heptanone-etheno-dGuo on system 3 were 13.3 and 20.6 min, respectively.

Preparation of Heptanone-etheno-methyl-dGuo and Carboxymethylnonanone-etheno-methyl-dGuo for NMR and LC/MS^n Analysis. After 36 h of incubation at 60 °C, the reaction mixture of 13(*S*)-HPODE, dGuo, and vitamin C was evaporated to dryness under nitrogen. The residue was redissolved with 200 μL of methanol and treated with 1.0 mL of ethereal diazomethane. The solution was allowed to stand for 1 h at room temperature, evaporated to dryness under nitrogen, and reconstituted in 200 μL of water. The aqueous solution was then applied to an SPE cartridge (1 g, 6 mL) that had been preconditioned with acetonitrile (10 mL) and water (10 mL). The cartridge was washed with water (10 mL) and 10% acetonitrile in water (10 mL). Methylated heptanone-etheno- and carboxynonanone-etheno-dGuo were eluted in acetonitrile (6 mL). The eluates was evaporated to dryness under nitrogen and dissolved in a 200 μL mixture of acetonitrile/water (2:8, v/v). After filtration with 0.2 μm Costar cartridge, methylated heptanone-etheno- and carboxynonanone-etheno-dGuo were isolated using gradient system 4, by monitoring the UV absorbance at 230 nm. The fractions containing methylated dGuo adducts (as determined by LC/MS) were combined, concentrated under nitrogen with adding CCl_4 as an azeotropic solvent, and dried under vacuum, respectively. The retention times of pure heptanone-etheno-methyl-dGuo and carboxymethylnonanone-etheno-methyl-dGuo on system 4 were 13.8 and 15.6 min, respectively.

Preparation of Heptanone-etheno-^{13}C-methyl-dGuo for NMR Analysis. Iodomethane-^{13}C (1.6 mmol) and 20% DIPE in acetonitrile (40 μL) were added to pure heptanone-etheno-dGuo (0.4 μmol) in acetonitrile (100 μL). The reaction mixture was vortex mixed for 1 min and incubated at room temperature for 1 h. After evaporation to dryness under nitrogen, the residues were redissolved in a 100 μL mixture of acetonitrile/water (2:8, v/v). Heptanone-etheno-^{13}C-methyl-dGuo (retention time, 13.8 min) was isolated using gradient system 4, by monitoring the UV absorbance at 230 nm.

Reaction of DODE with dGuo and Methylation of the Reaction Mixture. A solution of DODE (0.88 μmol) in ethanol (20 μL) was added to dGuo (6.45 μmol) in Chelex-treated 100 mM MOPS containing 150 mM NaCl (pH 7.4, 230 μL). The reaction mixture was sonicated for 15 min at room temperature, incubated at 37 °C for 24 h, and then placed on ice. The sample was filtered through a 0.2 μm Costar cartridge prior to analysis of a portion of the sample (20 μL) by LC/MS using gradient system 3. Methylation of reaction mixture was performed with ethereal diazomethane solution as described above and analyzed by LC/MS using gradient system 3.

Results

Vitamin C-Mediated Decomposition of 13-HPODE in the Presence of dGuo. LC/APCI/MS analysis of the reaction mixture revealed three major adducts (Figure 1A). The mass spectrum of the earliest eluting adduct (10.0 min) (Figure 1A, upper) revealed an intense protonated molecular ion [MH^+] at *m/z* 292, together with a BH_2^+ ion at *m/z* 176. MS^2 analysis of MH^+ resulted in

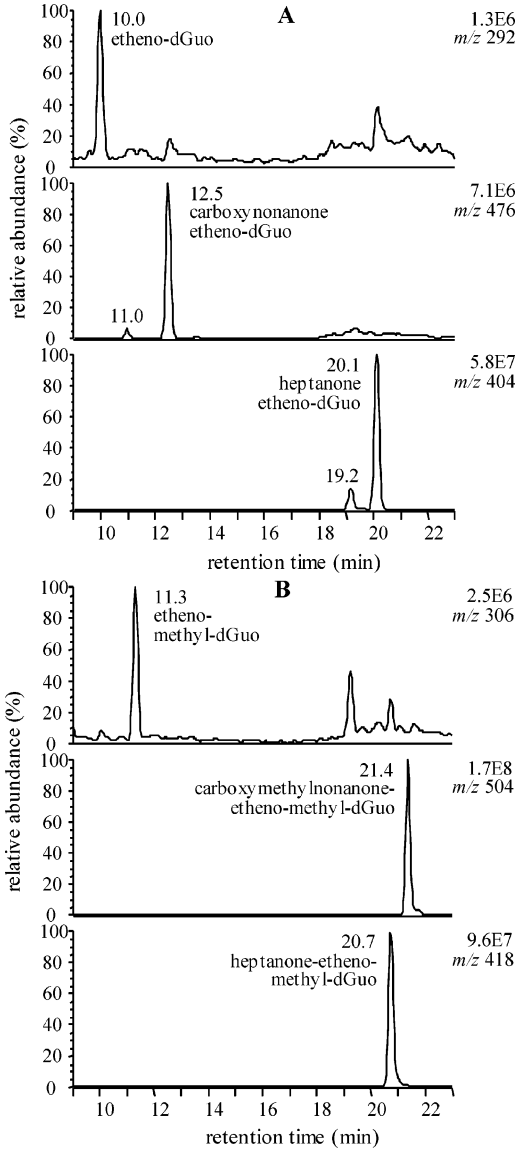

Figure 1. Analysis of the reaction between 13-HPODE and dGuo for 24 h at 37 °C using gradient system 3. LC/MS chromatogram showing the reconstructed selected ion chromatograms for the MH^+ of etheno-dGuo (top), carboxynonanone-etheno-dGuo (middle), and heptanone-etheno-dGuo (lower). (A) Before methylation and (B) after methylation.

a BH_2^+ product ion. These LC/MS characteristics were identical to those for etheno-dGuo. LC/MS analysis of the most abundant adduct (20.1 min) showed an MH^+ at *m/z* 404, together with BH_2^+ at *m/z* 288. MS^2 analysis of MH^+ gave rise to an intense BH_2^+ ion. Further CID of the BH_2^+ ion at *m/z* 288 (MS^3) gave rise to ions at *m/z* 190 ($BH_2^+ - C_5H_{11}CO$) and *m/z* 260. These mass spectral characteristics were consistent with heptanone-etheno-dGuo. The small peak (19.2 min) that eluted prior to heptanone-etheno-dGuo (Figure 1A, lower) was identified as heptanone-ethano-dGuo (MH^+, *m/z* 422; BH_2^+, *m/z* 306) (*13*). The dGuo adduct that eluted at 12.5 min had an MH^+ at *m/z* 476 and a BH_2^+ ion at *m/z* 360 (Figure 1A, middle), which corresponded to carboxynonanone-etheno-dGuo consistent with structure **A2** or **B2** in Scheme 3. Carboxynonanone-ethano-dGuo (consistent with structure **A1** or **B1** in Scheme 3) was also observed as a small peak at a retention time of 11.0 min. It had an MH^+ at *m/z* 494 and a BH_2^+ ion at *m/z* 378 (data not shown).

Scheme 3. Potential Structures of Carboxynonanone-ethano- and Carboxynonanone-etheno-dGuo Adducts and Bis-methylated Derivatives: N^2, $N1$ dGuo Regioisomers A1, A2, and A3 and $N1$, N^2 dGuo Regioisomers B1, B2, and B3

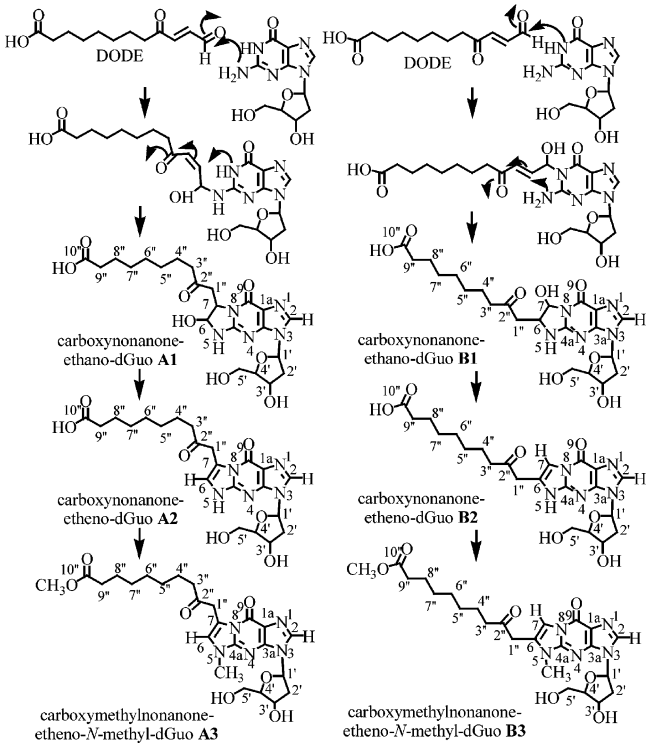

Methylation of the Reaction Mixture of 13-HPODE and dGuo. A weak response of carboxynonanone-etheno-dGuo was observed under positive APCI conditions. Therefore, the reaction mixture was methylated with diazomethane in order to improve its ionization characteristics. After methylation, LC/MS analysis in the positive APCI mode showed the expected MH^+ ions at *m/z* 306 for E-dGuo (11.3 min) and at *m/z* 418 for heptanone-etheno-dGuo (20.7 min) as mono-methyl derivatives (Figure 1B). LC/MS analysis of methylated carboxynonanone-etheno-dGuo revealed a substantial shift in retention time (12.5−21.4 min) and an intense MH^+ ion at *m/z* 504 corresponding to an increase in mass of 28 Da, suggesting that two methyl groups had been introduced (Figure 1B).

LC/MS^n Analysis of Carboxynonanone-etheno-dGuo. The mass spectrum of carboxynonanone-etheno-dGuo exhibited an intense MH^+ ion at *m/z* 476 together with a BH_2^+ ion at *m/z* 360 (Figure 2A). MS^2 analysis of MH^+ resulted in the exclusive formation of the BH_2^+ product ion at *m/z* 360 (Figure 2B). CID of *m/z* 360 (MS^3) gave rise to product ion at *m/z* 342 ($-H_2O$) (Figure 2C), which produced an intense ion at *m/z* 314 ($-CO$) from MS^4 analysis (Figure 2D). Finally, CID of *m/z* 314 (MS^5) gave rise to product ions at *m/z* 296 ($-H_2O$), *m/z* 244 ($-C_5H_{10}$), *m/z* 216 ($-C_7H_{14}$), and *m/z* 190 ($-C_7H_{14}CO$ + 2H) (Figure 2E). These mass spectral characteristics were consistent with the substituted etheno-dGuo adduct structure that contained a carboxyl group on its side chain. The MS^3 and MS^4 analyses revealed the presence of a carboxyl group and the MS^5 analysis showed the presence of a nonanone moiety.

LC/MS^n Analysis of Carboxymethylnonanone-etheno-methyl-dGuo. The MS^n spectra of carboxy-

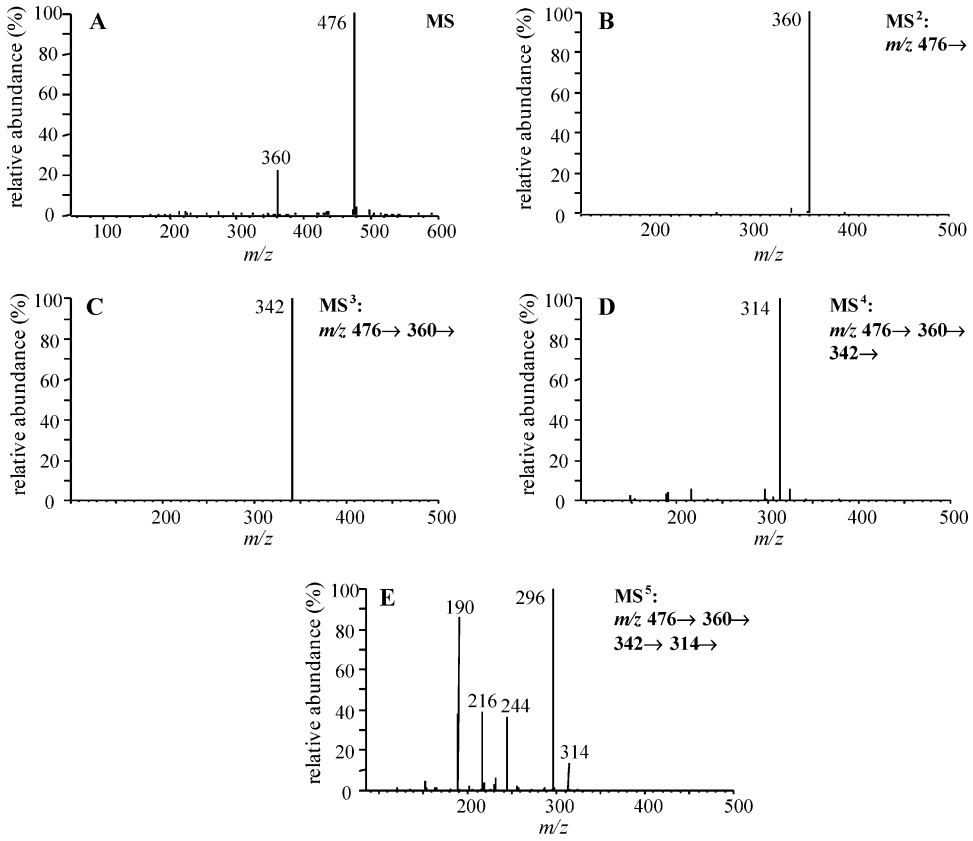

Figure 2. LC/MS^n analysis of carboxynonanone-etheno-dGuo. (A) Full-scan mass spectrum, (B) MS^2 spectrum, (C) MS^3 spectrum, (D) MS^4 spectrum, and (E) MS^5 spectrum.

Table 1. ^{1}H NMR Assignments for Heptanone-etheno-methyl-dGuo[a]

assigned H	δ (ppm)	multiplicity	H-coupled (J Hz)	type
H-2	8.07	s		N=C*H*−
H-6	7.20	s	H-1″	C=C*H*
H-1′	6.27	t	H-2′a (7.1), H-2′b (7.1)	*N*−C*H*−O
3′-OH	5.31	bs		−CHO*H*
5′-OH	4.91	bs	H-5′a, H-5′b	−CH_2O*H*
H-3′	4.39	m	H-2′a, H-2′b, H-4′	−O−C*H*−
H-1″a,b	4.13	s		−CH_2−C
H-4′	3.84	m	H-3′, H-5′a, H-5′b	−O−C*H*−
NCH_3 or *O*CH_3	3.60	s		−*N*−CH_3 or −*O*−CH_3
H-5′b	3.58	m	H-4′, H-5′a, 5′-OH	−CH_2−O
H-5′a	3.51	m	H-4′, H-5′b, 5′-OH	−CH_2−O
H-2′b	2.66	m	H-1′, H-2′a, H-3′	−CH_2−C
H-3″a,b	2.55	t	H-4″a (7.4), H-4″b (7.4)	−CH_2−C
H-2′a	2.25	m	H-1′, H-2′b, H-3′	−CH_2−C
H-4″a,b	1.50	m	H-3″a,b, H-5″a,b	−CH_2−C
H-6″a,b	1.26	m	H-5″a, H-5″b, H-7″	−CH_2−C
H-5″a,b	1.25	m	H-4″a, H-4″b, H-6″a, H-6″b	−CH_2−C
H-7″	0.86	t	H-6″a (7.0), H-6″b (7.0)	−CH_3

[a] Spectra were obtained in DMSO-d_6.

methylnonanone-etheno-methyl-dGuo showed the same pattern to that obtained for underivatized carboxynonanone-etheno-dGuo. The MS spectrum exhibited an intense MH^+ ion at *m/z* 504 together with a BH_2^+ ion at *m/z* 388, corresponding to its bis-methyl derivative. Consecutive MS^5 analysis revealed positions of two methyl groups: *m/z* 504 (MH^+) → *m/z* 388 (BH_2^+) → *m/z* 356 (−CH_3OH) → *m/z* 328 (−CO) → *m/z* 310 (−H_2O), *m/z* 258 (−C_5H_{10}), *m/z* 230 (−C_7H_{14}), and *m/z* 204 (−C_7H_{14}-CO + 2H). The presence of the methyl ester from the carboxymethylnonanone side chain was confirmed from MS^3 analysis [*m/z* 388 (BH_2^+) → *m/z* 356 (−CH_3OH)]. The other methyl group was not lost during CID, suggesting that it was attached to the etheno-dGuo structure.

NMR Analysis of Heptanone-etheno-methyl-dGuo. The aromatic proton singlet at 7.20 ppm (H-6) (Table 1) showed a COSY correlation with the methylene protons at C-1″ (4.13 ppm). This was consistent with the presence of an olefinic bond between C-6 and C-7 in structures **C1**, **C2**, **D1**, and **D2** (Scheme 4). The triplet at 2.55 ppm was assigned to the methylene protons at C-3″ based on its chemical shift and its multiplicity (Table 1). The COSY spectrum showed correlations of the C-3″ protons with the C-4″ protons (1.50 ppm), the C-4″ protons with the C-5″ protons (1.25 ppm), the C-5″ protons with the C-6″ protons (1.26 ppm), and finally, the C-6″ protons with the methyl group at C-7″ (0.86 ppm). The COSY spectrum also showed the correlations of the protons of the fura-

Scheme 4. Potential Structures of Methylated Heptanone-etheno-dGuo Adducts: N^2, $N1$ dGuo Regioisomers C1 and C2 and $N1$, N^2 dGuo Regioisomers D1 and D2

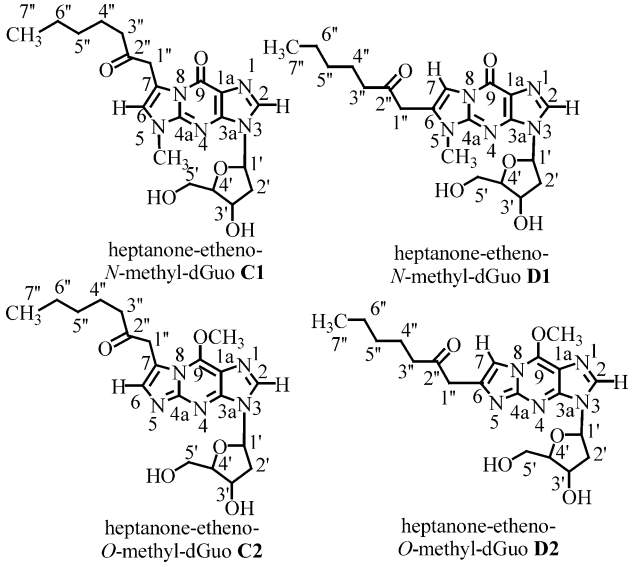

nosyl moiety. ^{1}H NMR analysis revealed that the chemical shift of the methyl group was at 3.60 ppm (Table 1), which made it difficult to determine whether it resulted from *O*- or *N*-methylation. ^{1}H chemical shifts of *N*-CH_3 groups have been obtained from ^{1}H NMR analysis of pyrroles (δ 3.60 ppm), imidazoles (δ 3.60 ppm), and fused pyrrole rings (δ 4.33 ppm) (*42*). The ^{1}H chemical shift of *O*-CH_3 would be expected at 3.70 ppm (*43*). The HSQC experiment showed a ^{13}C chemical shift of 30.9 ppm (Table 2). ^{13}C chemical shifts of *N*-CH_3 derivatives have been obtained from ^{13}C NMR analysis of pyrroles (δ 35.2 ppm), imidazoles (δ 32.6 ppm), and fused pyrrole rings (δ 27.8 ppm) (*44*). The ^{13}C chemical shift of *O*-CH_3 would be expected downfield at 54 ppm (*44*). Therefore, ^{1}H and ^{13}C NMR spectra were consistent with the presence of an *N*-methyl group in heptanone-*N*-methyl-dGuo (**C1**) rather than an *O*-methyl group as in heptanone-*O*-methyl-dGuo (**C2**) (Scheme 4). H-2 and its site of attachment (C-2) were assigned based on the three-bond C−H long-range correlations C-2/H-1′, C-1a/H-2, and C-3a/H-2 from the HMBC spectrum, and its one-bond C−H correlation C-2/H-2 from the HSQC spectrum. H-6 and its site of attachment (C-6) were assigned based on the three-bond C−H long-range correlations C-6/H-1″ and C-4a/H-6, the two-bond C−H correlation C-7/H-6 from the HMBC spectra, and its one-bond correlation C-6/H-6 from the HSQC spectrum.

Table 2. ^{13}C NMR Assignments for Heptanone-etheno-methyl-dGuo[a]

assigned carbon	δ (ppm)	coupling	type
C-7″	13.5		−*C*H$_3$
C-6″	21.6	H-4″, H-5″, H-7″	−*C*H$_2$−
C-4″	22.3	H-3″	−*C*H$_2$−
C-5″	30.6	H-3″, H-4″, H-6″, H-7″	−*C*H$_2$−
N-CH_3	30.9		*N*-*C*H$_3$
C-2′	38.7		−*C*H$_2$−
C-1”	39.0		−*C*H$_2$−
C-3”	40.8	H-4″	−*C*H$_2$−
C-5′	61.5		−*C*H$_2$−O
C-3′	70.6	H-2′	−*C*H−O
C-1′	82.9	H-2′	N−*C*HO−
C-4′	87.5		−*C*HO
C-1a	115.8	H-2	C=*C*−N
C-7	116.6	H-1″	C=*C*−N
C-6	119.0	H-1″, *N*-CH_3	−*N*−*C*H=C
C-2	137.2	H-1′	−N−*C*H=N
C-4a	145.6	H-6, *N*-CH_3	−N−*C*=N
C-3a	149.3	H-2, H-1′	N−*C*=N
C-9	NA		
C-2″	205.4	H-1″, H-3″, H-4″	−*C*=O

[a] Spectra were obtained in DMSO-d_6. Couplings were obtained from the HMBC plot.

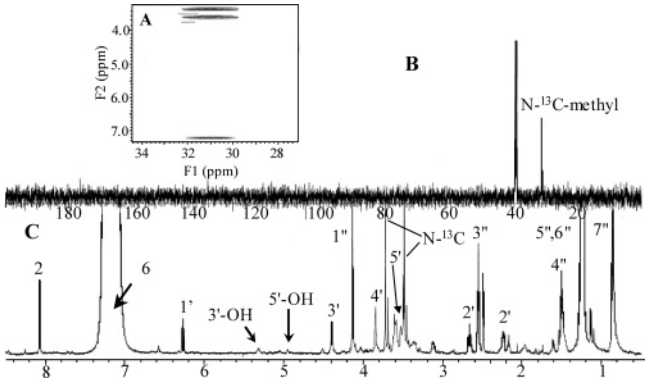

Figure 3. Spectra of heptanone-etheno-^{13}*C*-methyl-dGuo (DMSO-d_6, 600 MHz). (A) HMBC, (B) ^{13}C NMR, and (C) ^{1}H NMR.

The ROESY experiment showed a nuclear Overhauser effect (NOE) between the methyl group and the aromatic proton at 7.20 ppm, which allowed two possibilities for the attachment of the heptane-2″-one side chain, one where the methyl group is attached to *N*-5 and the aromatic proton is at H-6 (**C1** and **D1**; Scheme 4) and the other where the methyl group is at *O*-9 and the aromatic proton is at H-7 (**C2** and **D2**; Scheme 4). HMBC experiments were performed at three different long-range C−H coupling constants (J = 5, 7, and 10 Hz) to avoid missing correlations. To avoid misinterpretation of the position of the methyl group from the HMBC data, a synthetic enriched ^{13}*C*-methyl sample was prepared. The ^{1}H NMR spectrum (Figure 3C) showed the labeled methyl group as a doublet with a coupling constant of 141.5 Hz and as a singlet in the ^{13}C NMR spectrum (Figure 3B). The HMBC experiment (Figure 3A) showed the ^{13}*C*-methyl carbon correlated to its attached protons and to H-6 indicating that it was attached to *N*-5 (three bonds). If the ^{13}*C*-methyl group had been attached to *O*-9 as shown in structures **C2** and **D2** in Scheme 4, the HMBC experiment would not have detected a correlation between the methyl carbon and the H-6 vinylic proton at 7.20 ppm (six bonds). Similarly, if the ^{13}C-methyl group had been attached to *O*-9 in structures **C2** and **D2** of Scheme 4, there would have been no correlation between the methyl carbon and a vinyl proton at H-7 (five bonds). This ruled out the possibility of *O*-methylation. Further HMBC analysis revealed a correlation of the methyl protons at 3.60 ppm with the signals at 119.0 and 145.6 ppm, which corresponded to C-6 and C-4a, respectively. This unequivocally established that the methyl group was at *N*-5 as in **C1** and **D1** rather than *O*-9 as in **C2** or **D2** (Scheme 4). Structure **C1** was favored over **D1** because it was consistent with the HMBC data. The *N*-methyl group in structure **C1** is only three bonds away from the vinyl hydrogen at C-6 (Scheme 4) as compared with being four bonds away from the vinyl hydrogen at C-7 in structure **D1** (Scheme 4). The chemical shift of C-9 was not detected by HMBC; therefore, the assignment of a carbonyl or hydroxy moiety at C-9 remains somewhat

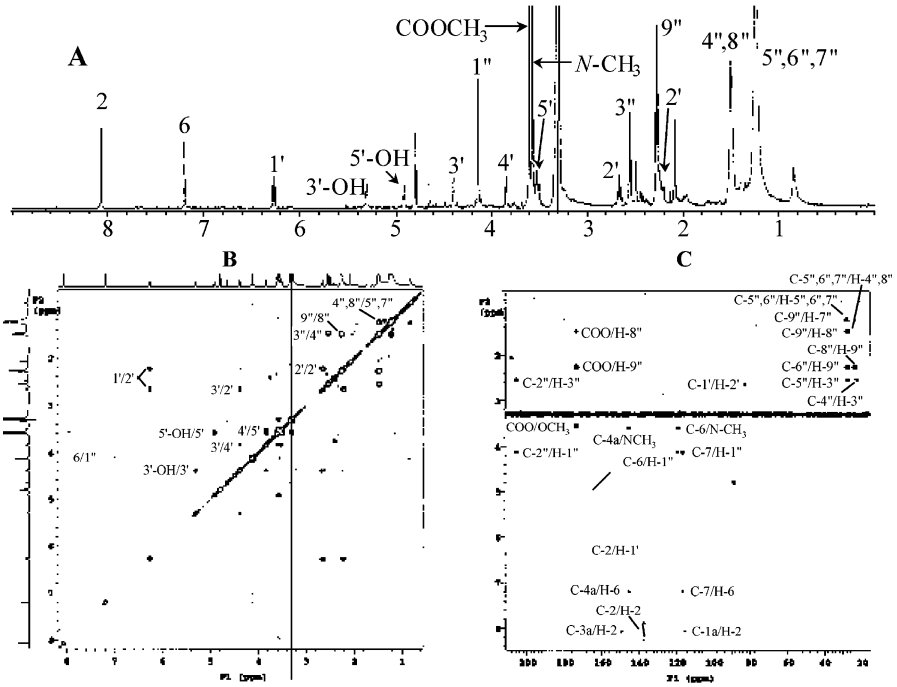

Figure 4. Spectra of carboxymethylnonanone-etheno-methyl-dGuo (DMSO-d_6, 600 MHz). (A) ^{1}H NMR, (B) COSY, and (C) HMBC.

Table 3. ^{1}H NMR Assignments for Carboxymethylnonanone-etheno-methyl-dGuo[a]

assigned H	δ (ppm)	multiplicity	H-coupled (J Hz)	type
H-2	8.07	s		N=C*H*−
H-6	7.20	s		C=C*H*
H-1′	6.27	t	H-2′a (7.0), H-2′b (7.0)	N−C*H*−O
3′-OH	5.30	bd	H-3′ (3.8)	−CHO*H*
5′-OH	4.91	bt	H-5′a (5.5), H-5′b (5.5)	−CH_2O*H*
H-3′	4.39	m	H-2′a, H-2′b, H-4′	−O−C*H*−
H-1″a,b	4.13	s		−CH_2−C
H-4′	3.84	m	H-3′, H-5′a, H-5′b	−O−C*H*−
N-CH_3	3.60	s		−*N*−CH_3
H-5′b	3.58	m	H-4′, H-5′a, 5′-OH	−CH_2−O
O−CH_3	3.56	s		−COOCH_3
H-5′a	3.51	dd	H-4′ (5.5), H-5′b (11.8), 5′-OH	−CH_2−O
H-2′b	2.66	m	H-1′, H-2′a, H-3′	−CH_2−C
H-3″a,b	2.55	t	H-4″a (7.3), H-4″b (7.3)	−CH_2−C
H-2′a	2.23	ddd	H-1′ (7.0), H-2′b (13.2), H-3′ (2.8)	−CH_2−C
H-9″a,b	2.27	t	H-8″a (7.4), H-8″b (7.4)	−CH_2−C
H-4″a,b	1.50	m	H-3″a, H-3″b, H-5″a, H-5″b	−CH_2−C
H-8″a,b	1.50	m	H-7″a, H-7″b, H-9″a, H-9″b	−CH_2−C
H-5″	1.25	m	H-4″a, H-4″b, H-6″a, H-6″b	−CH_2−C
H-6″	1.25	m	H-5″a, H-5″b, H-7″a, H-7″a	−CH_2−C
H-7″	1.25	m	H-6″a, H-6″b, H-8″a, H-8″b	−CH_2−C

[a] Spectra were obtained in DMSO-d_6.

tentative. These data are consistent with the structural assignment of heptanone-etheno-methyl-dGuo as the *N*-methyl derivative 3-(2′-deoxy-β-D-erythropentafurano-syl)imidazo-7-(heptane-2″-one)-9-oxo-5-*N*-methyl[1,2-*a*]-purine (**C1**) rather then its *O*-methyl isomer (**C2**) or alternative potential regioisomers **D1** and **D2**.

NMR Analysis of Carboxymethylnonanone-etheno-methyl-dGuo. The presence of an olefinic bond between C-6 and C-7 consistent with structures **A3** or **B3** (Scheme 3) was confirmed by a COSY correlation between an aromatic proton singlet at 7.20 ppm for H-6 (**A3**; Scheme 3) or H-7 (**B3**; Scheme 3) and methylene protons at C-1″ (4.13 ppm) (Figure 4A,B). The triplet at 2.55 ppm was assigned to the methylene protons at C-3″ because of its chemical shift and its multiplicity (Figure 4A). The COSY spectrum showed correlations of the C-3″ protons (2.55 ppm) through C-9″ protons (2.27 ppm) (Figure 4B). The methylene protons at C-6″ and C-7″ overlapped with the protons at C-5″ (Figure 4A). The COSY spectrum showed the expected correlations for the protons of the furanosyl moiety. This spectrum also showed correlations between proton H-1′ (6.27 ppm) and the protons at C-2′ (2.66 and 2.23 ppm), the C-2′ protons with the C-3′ proton (4.39 ppm), the C-3′ protons with the C-4′ proton (3.84 ppm) and with the hydroxyl at C-3′ (5.30 pm), the C-4′ proton with the C-5′ protons (3.58 and 3.51 ppm), and the C-5′ protons with the hydroxyl at C-5′ (4.91 ppm) (Figure 4B). There are two methyl groups present as follows: one as a methyl ester with 3.56 and 51.0 ppm for the ^{1}H and ^{13}C chemical shifts, respectively (Tables 3 and 4), and the other, which was confirmed to be an *N*-methyl group by the HMBC experiment (Figure 4C), had ^{1}H and ^{13}C chemical shifts at 3.60 and 31.2 ppm, respectively (Tables 3 and 4). The ROESY experiment showed an NOE between the methyl group at 3.60 ppm and the aromatic proton at 7.20 ppm, which allows two

Table 4. ^{13}C NMR Assignments for Carboxymethylnonanone-etheno-methyl-dGuo[a]

assigned carbon	δ (ppm)	coupling	type
C-4″	22.6	H-3″	$-CH_2-$
C-8″	24.1	H-9″	$-CH_2-$
C-5″	28.3	H-3″, H-4″, H-6″, H-7″	$-CH_2-$
C-6″	28.3	H-5″, H-7″, H-8″, H-9″	$-CH_2-$
C-7″	28.3		$-CH_2-$
N-CH_3	31.2		$N-CH_3$
C-9″	33.0	H-7″, H-8″	$-CH_2-$
C-2′	38.7		$-CH_2-$
C-1″	39.1		$-CH_2-$
C-3″	40.8		$-CH_2-$
$COOCH_3$	51.0		$-COOCH_3$
C-5′	61.7		$-CH_2-O$
C-3′	70.9		$-CH-O$
C-1′	83.0	H-2′	$N-CHO-$
C-4′	87.5		$-CHO$
C-1a	116.0	H-2	$C=C-N$
C-7	116.8	H-6	$C=C-N$
C-6	119.1	H-1″, $N-CH_3$	$-N-CH=C$
C-2	137.3	H-1′	$-N-CH=N$
C-4a	145.7	H-6, $N-CH_3$	$-N-C=N$
C-3a	149.3	H-2	$N-C=N$
C-9	NA		
$COOCH_3$	173.3	H-8″, H-9″, $O-CH_3$	$-COOCH_3$
C-2″	205.5	H-1″, H-3″	$-C=O$

[a] Spectra were obtained in DMSO-d_6. Couplings were obtained from the HMBC plot.

possibilities for the attachment of the 9″-carboxynona-2″-one side chain, one where the methyl group is attached to *O*-9 and the aromatic proton is at H-7 (**B3**; Scheme 3), and the second where the methyl group is attached N-5 and the aromatic proton is at H-6 (**A3**; Scheme 3). The HMBC assignments of C-1a (116.0 ppm), C-3a (149.3 ppm), and C-4a (145.7 ppm) through the H-2/C-1a, H-2/C-3a, and H-6/C-4a were essential for this analysis. HMBC showed a correlation of the methyl protons at 3.60 ppm with the signals at 119.1 and 145.7 ppm, which corresponded to C-6 and C-4a, respectively (three bonds), and confirmed that the methyl group was at *N*-5 (**A3**; Scheme 3). These data also eliminated the possible alternative regioisomeric structure **B3** shown in Scheme 3 because a correlation of the *N*-5 methyl protons with C-7 would have required an HMBC interaction through four bonds in structure **B3** when compared with the three bonds from *N*-5 to C-6 in structure **A3**. On the basis of these data, the structure of carboxymethylnonanone-etheno-*N*-methyl-dGuo was assigned as 3-(2′-deoxy-β-D-erythropentafuranosyl)imidazo-7-(9″-carboxymethylnona-2″-one)-9-oxo-5-*N*-methyl[1,2-*a*]purine (**A3**).

NMR Analysis of Carboxynonanone-etheno-dGuo. The aromatic proton singlet at 7.13 ppm (H-6) (Figure 5A and Table 5) showed a weak COSY correlation with the methylene protons at C-1″ (4.12 and 4.09 ppm) (Figure 5B). This was consistent with the presence of an olefinic bond between C-6 and C-7 (**A2** and **B2**; Scheme 3). The COSY spectrum showed correlations between the C-3″ protons with the C-4″ protons (1.48 ppm) and the C-4″ protons with the C-5″ protons (1.25 ppm) (Figure 5B). The methylene protons at C-6″ and C-7″ overlapped with the protons at C-5″ (Figure 5A). The COSY spectrum also showed correlations of the protons from the furanosyl moiety. The ROESY spectrum indicated rotation of the N3−C1′ bond based on the NOEs between protons at C-2 with H-1′, H-2′, and H-3′ from the furanosyl moiety. HMBC analysis (Figure 5C) showed the most important correlations that were essential for structural assignment (Table 6): C-1a (115.8 ppm), C-3a (149.7 ppm), and C-4a (146.6 ppm) through the H-2/C-1a, H-2/C-3a, and H-6/C-4a. Therefore, the structure of carboxynonanone-etheno-dGuo was assigned as 3-(2′-deoxy-β-D-erythropentafuranosyl)imidazo-7-(9″-carboxynona-2″-one)-oxo-[1,2*a*]purine (**A2**) rather than the alternative regioisomeric structure **B2**.

UV Analysis of Carboxynonanone-etheno-dGuo. The UV spectrum of carboxynonanone-etheno-dGuo showed the same reversible pH dependence as heptanone-etheno-dGuo (*13*) and heptanone-etheno-dAdo (*15*). It exhibited a λ_{max} of 230 nm ($\epsilon = 9270$ M^{-1} cm^{-1}) at pH 7 (Figure 6). The λ_{max} was shifted to 237 nm ($\epsilon = 9750$

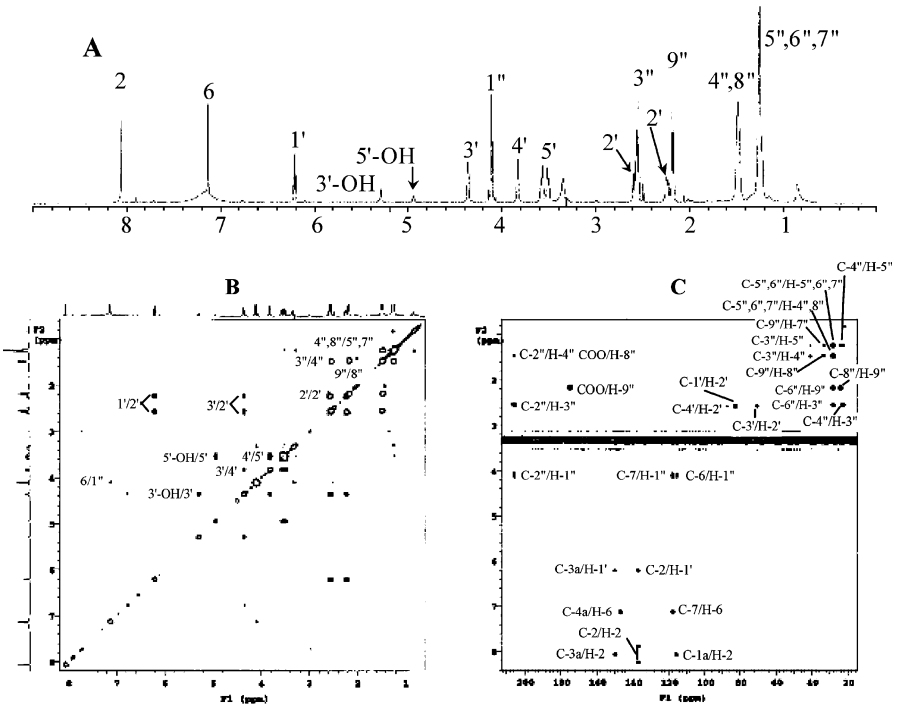

Figure 5. Spectra of carboxynonanone-etheno-dGuo (DMSO-d_6, 600 MHz). (A) ^{1}H NMR, (B) COSY, and (C) HMBC.

Table 5. ^{1}H NMR Assignments for Carboxynonanone-etheno-dGuo[a]

assigned H	δ (ppm)	multiplicity	H-coupled (J Hz)	type
H-2	8.06	s		N=C*H*−
H-6	7.13	s	H-1″	C=C*H*
H-1′	6.21	t	H-2′a (6.8), H-2′b (6.8)	N−C*H*−O
3′-OH	5.23	bd	H-3′ (3.6)	−CHO*H*
5′-OH	4.94	bs	H-5′a, H-5′b	−CH_2O*H*
H-3′	4.36	m	H-2′a, H-2′b, H-4′	−O−C*H*-
H-1″b	4.12	d	H-1″a (17.9)	−CH_2−C
H-1″a	4.09	d	H-1″b (17.9)	−CH_2−C
H-4′	3.83	m	H-3′, H-5′a, H-5′b	−O−C*H*-
H-5′b	3.57	m	H-4′, H-5′a, 5′-OH	−CH_2−O
H-5′a	3.51	dd	H-4′ (5.5), H-5′b (11.8), 5′-OH	−CH_2−O
H-2′b	2.58	m	H-1′, H-2′a, H-3′	−CH_2−C
H-3″a,b	2.55	t	H-4″a (7.4), H-4″b (7.4)	−CH_2−C
H-2′a	2.24	ddd	H-1′ (5.8), H-2′b (13.0), H-3′ (3.1)	−CH_2−C
H-9″a,b	2.18	t	H-8″a (7.3), H-8″b (7.3)	−CH_2−C
H-4″a,b	1.48	m	H-3″a, H-3″b, H-5″a, H-5″b	−CH_2−C
H-8″a,b	1.48	m	H-7″a, H-7″b, H-9″a, H-9″b	−CH_2−C
H-5″	1.25	m	H-4″a, H-4″b, H-6″a, H-6″b	−CH_2−C
H-6″	1.25	m	H-5″a, H-5″b, H-7″a, H-7″a	−CH_2−C
H-7″	1.25	m	H-6″a, H-6″b, H-8″a, H-8″b	−CH_2−C

[a] Spectra were obtained in DMSO-d_6.

Table 6. ^{13}C NMR Assignments for Carboxynonanone-etheno-dGuo[a]

assigned carbon	δ (ppm)	coupling	type
C-4″	22.7	H-3″, H-5″	−*C*H_2−
C-8″	24.1	H-7″, H-9″	−*C*H_2−
C-5″	28.3	H-4″, H-6″, H-7″	−*C*H_2−
C-6″	28.3	H-5″, H-7″, H-8″	−*C*H_2−
C-7″	28.3		−*C*H_2−
C-9″	33.4	H-7″, H-8″	−*C*H_2−
C-2′	39.2	3′-OH	−*C*H_2−
C-1″	39.4		−*C*H_2−
C-3″	40.9	H-4″, H-5″	−*C*H_2−
C-5′	61.5	5′-OH	−*C*H_2−O
C-3′	70.5	H-2′, H-5′, 3′-OH	−*C*H−O
C-1′	82.9	H-2′	*N*−*C*HO−
C-4′	87.5	H-2′, H-5′, 3′-OH, 5′-OH	−*C*HO
C-6	115.4	H-1″	−N−*C*H=C
C-1a	115.8	H-2	C=*C*−N
C-7	117.8	H-6, H-1″	C=*C*−N
C-2	136.7	H-1′	−N−*C*H=N
C-4a	146.6	H-6	−N−*C*=N
C-3a	149.7	H-2, H-1′	N−*C*=N
C-9	NA		
COOH	174.5	H-8″, H-9″	−*C*OOH
C-2″	205.7	H-1″, H-3″, H-4″	−*C*=O

[a] Spectra were obtained in DMSO-d_6. Couplings were obtained from the HMBC plot.

M^{-1} cm^{-1}) at pH 13 and to 227 nm (ϵ = 7730 M^{-1} cm^{-1}) at pH 1.

Large Scale Preparation of DODE. An efficient route for the synthesis of DODE was developed starting from 1,8-octanediol. The overall synthetic scheme was based on methodology developed by the Salomon group (*39*, *40*) (Scheme 5). Protection of one hydroxyl group in 1,8-octanediol as a TBDMS ether derivative (**1**) was followed by bromination (**2**), attachment of the THF, and deprotection of the alcohol (**3**). This was followed by oxidation to the terminal carboxylate (**4**) and treatment with NBS to give DODE as its 10(*E*)-stereoisomer (**5**) with >99% purity (from LC/MS analysis) in an overall yield of 15% from **1**. The stereochemistry of the olefin was assigned as 10(*E*) rather than 10(*Z*) because the coupling constant between the olefinic protons at H-10 and H-11 was 16.0 Hz as compared with 12.4 Hz reported for the *Z*-isomer (*31*).

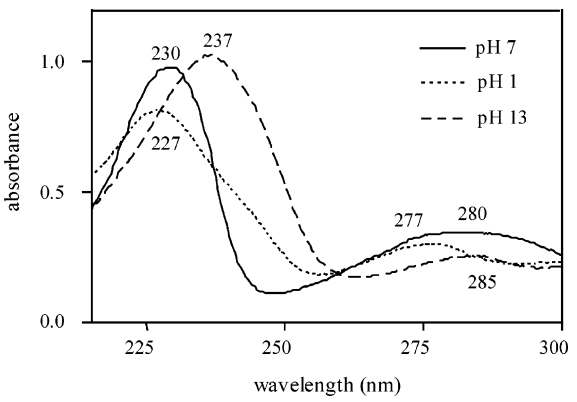

Figure 6. UV spectra of carboxynonanone-etheno-dGuo at pH 1, 7, and 13.

Reaction of DODE with dGuo and Methylation of Reaction Products. DODE was treated with dGuo in order to determine whether the same products were observed as in the reaction between 13-HPODE and

Scheme 5. Synthetic Route for the Preparation of DODE

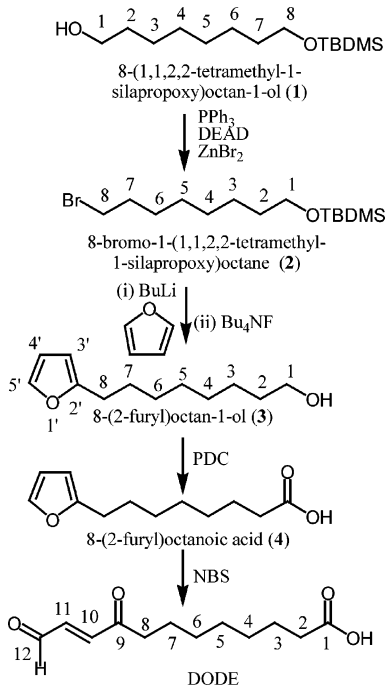

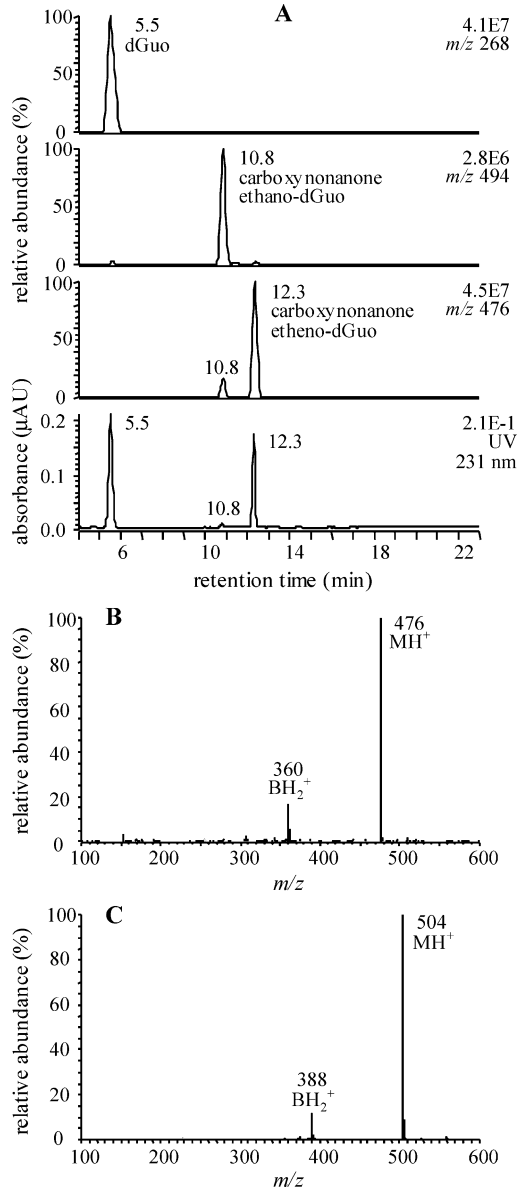

Figure 7. (A) Analysis of the reaction between DODE and dGuo for 24 h at 37 °C by concurrent LC/MS and UV detection using gradient system 3. The three upper panels are the reconstructed selected ion chromatograms for the MH^+ of dGuo (*m/z* 268), carboxynonanone-ethano-dGuo (*m/z* 494), and carboxynonanone-etheno-dGuo (*m/z* 476). The lower panel is the UV absorbance at 231 nm. (B) Full-scan spectrum of peak at 12.3 min (carboxynonanone-etheno-dGuo). (C) Full-scan spectrum of carboxynonanone-etheno-dGuo after methylation.

dGuo. LC/MS analysis of the products from the reaction between synthetic DODE and dGuo at 37 °C for 24 h revealed the presence of one major compound with MH^+ at *m/z* 476 (carboxynonanone-etheno-dGuo) and one minor compound with MH^+ at *m/z* 494 (carboxynonanone-ethano-dGuo) (Figure 7A). Residual dGuo (MH^+; *m/z* 268) was also observed. The LC effluent was allowed to pass through a UV detector (231 nm) prior to mass spectrometer. The resulting chromatogram confirmed the presence of two products together with residual dGuo. The MS (Figure 7B) and MS^n characteristics of the major compound that eluted at 12.3 min were identical with carboxynonanone-etheno-dGuo, which was identified from the reaction of 13-HPODE with dGuo. After methylation, the identity of major compound was further confirmed by LC/MS (Figure 7C) and MS^n analyses.

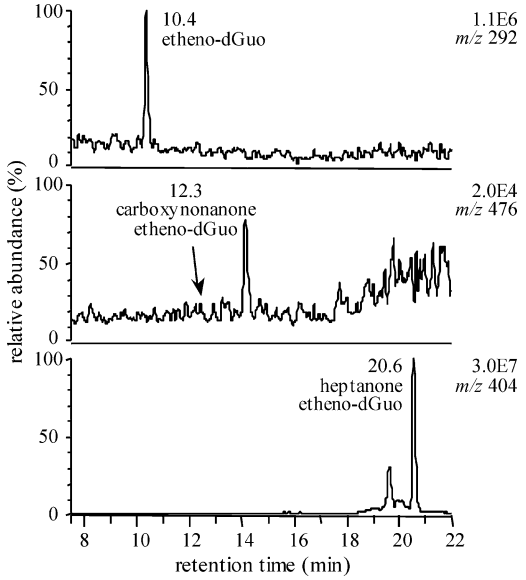

Figure 8. Analysis of the reaction between 15-HPETE and dGuo for 24 h at 37 °C using gradient system 3. LC/MS chromatogram showing the reconstructed selected ion chromatograms for the MH^+ of etheno-dGuo (top), carboxynonanone-etheno-dGuo (middle), and heptanone-etheno-dGuo (lower).

Vitamin C-Mediated Decomposition of 15-HPETE in the Presence of dGuo. LC/MS analysis of the reaction mixture revealed the presence of etheno-dGuo (10.4 min) with MH^+ at *m/z* 292 and heptanone-etheno-dGuo (20.6 min) with MH^+ at *m/z* 404 (Figure 8). However, carboxynonanone-etheno-dGuo was not detected in the reaction mixture. The minor peak, which appeared at 14.1 min in the *m/z* 476 channel, was present in control incubations that contained no 15-HPETE or dGuo. Therefore, the compound that gives rise to this signal appears to be present in one of the other reagents. These data suggested that carboxynonanone-etheno-dGuo is a specific DNA adduct formed only from homolytic decomposition of 13-HPODE.

Discussion

DODE contains four electrophilic sites so that when it interacts with a bifunctional nucleophile such as dGuo numerous potential structural isomers can arise. It is particularly difficult to distinguish between initial nucleophilic attack of the exocyclic amine group N^2 of dGuo at the C-12 aldehyde from attack of the dGuo pyrimidine $N1$ at the C-12 aldehyde (Scheme 3). Each reaction provides a carbinolamine intermediate that is set up for intramolecular Michael addition to give ethano adducts **A1** or **B1** (Scheme 3). Subsequent dehydration as was observed with heptanone-ethano-dGuo adducts (*13*) would result in the formation of regioisomeric etheno adducts **A2** or **B2**. A potential pathway involving initial Michael addition at C-10 (as observed at the equivalent C-3 position of HNE) was ruled out because of the vinylic hydrogen singlet that was observed at 7.13 ppm in the resulting adduct (Table 5). This confirmed that an etheno rather than a propano derivative had been formed. In contrast, the addition of dGuo to HNE results in the formation of a propano adduct through an initial Michael addition at C-3 (*24*, *25*).

It was impossible to distinguish between the two potential DODE-derived etheno-dGuo regioisomers (**A2** and **B2** shown in Scheme 3) by NMR spectroscopy.

However, it was evident that this could be accomplished using HMBC analysis of the methyl-dGuo derivative if methylation occurred at *N*-5. Initial methylation experiments were conducted with ONE-derived heptanone-etheno-dGuo because extensive NMR characterization has already been performed (*13*), and so it provided a model for methylated DODE-derived adducts. The methyl group appeared at 3.60 ppm in the ^{1}H NMR spectrum of heptanone-etheno-methyl-dGuo (Table 1), which is in the range reported for both *N*-methyl and *O*-methyl derivatives (*42*, *43*). However, the ^{13}C chemical shift was 30.9 ppm (Table 2), which is more appropriate for an *N*-methyl group in **C1** or **D1** (*44*) than an *O*-methyl group as in **C2** or **D2** (*44*) (Scheme 4). HMBC demonstrated a correlation between the methyl group protons and H-6 at 7.20 ppm. This three-bond coupling confirmed that the methyl group was at *N*-5 as in **C1**. If the methyl group had been attached to *O*-9 as in **C2**, this correlation would not have been observed. The HMBC assignments were confirmed using ^{13}C-methylated heptanone-etheno-dGuo and confirmed its structure as the *N*-methylated derivative **C1** (Scheme 4).

Methylation of carboxynonanone-etheno-dGuo resulted in the formation of a bis-methylated derivative. The carboxymethyl group appeared at the expected chemical shifts of 3.56 and 51.0 ppm in the ^{1}H (Table 3) and ^{13}C NMR (Table 4) spectra, respectively. The other methyl group had chemical shifts in the ^{1}H NMR and ^{13}C NMR spectra that were almost identical with those observed in the methylated heptanone-etheno-dGuo at 3.60 ppm (Table 3) and 31.2 ppm (Table 4), respectively. This was consistent with *N*-methylation rather than *O*-methylation. HMBC assignments of C-1a (116.0 ppm), C-3a (149.3 ppm), and C-4a (145.7 ppm) through H-2/C-1a, H-2/C-3a, and H-6/C-4a were essential to assign the regioselective structure of carboxymethylnonanone-etheno-methyl-dGuo (Figure 4B). All three HMBCs showed a correlation of the methyl protons at 3.60 ppm with the ^{13}C NMR signals at 119.1 and 145.7 ppm, which corresponded to C-6 and C-4a, respectively (three bonds apart). The ROESY experiment showed an NOE between the methyl group at 3.60 ppm and the aromatic proton at 7.20 ppm. These data confirmed that the methyl group was at *N*-5 in structure **A3** and eliminated the possible alternative regioisomeric structure **B3** shown in Scheme 3. A correlation of the *N*-5 methyl protons with C-7 would have required an HMBC interaction through four bonds in structure **B3** when compared with the three bonds from *N*-5 to C-6 in structure **A3**. The structure of the DODE-derived dGuo adduct was established as **A2** because on methylation it was converted to **A3**.

Formation of regioisomer **A2** in Scheme 3 requires an initial reaction of the exocyclic N^2 of dGuo to the terminal aldehyde of DODE to form a carbinolamine intermediate. The NMR studies eliminated the possibility that Michael addition of *N*1 had occurred at C-12 to give carboxynonanone-etheno-dGuo regioisomer **B2**. After the initial reaction to form the carbinolamine intermediate, C-11 became the most electrophilic carbon. Therefore, intramolecular Michael addition of *N*1 occurred at this site to give an ethano derivative (**A1**). Subsequent dehydration provided the etheno-dGuo adduct **A2** that was subsequently converted to the bis-methyl derivative **A3**.

DODE has been synthesized previously as the 10(*Z*) isomer in order to characterize a linoleic acid-derived metabolite that was present in lentil seeds. This synthetic route is not amenable to the preparation of large quantities of the 10(*E*) isomer for use in studies of DNA and protein adduct formation and to study the role of DODE in oxidative stress. Therefore, we have developed an efficient synthesis of DODE based on methodology developed by the Salomon group (*39*, *40*) (Scheme 5). The reaction of synthetic DODE with dGuo produced a DNA adduct (carboxynonanone-etheno-dGuo), which was identical to that observed when 13(*S*)-HPODE was treated with vitamin C in the presence of dGuo. Extensive LC/MS studies were conducted to show that no other carboxynonanone-etheno-dGuo regioisomers were formed. Methylation of the carboxynonanone-etheno-dGuo improved its MS ionization characteristics by a factor of approximately 20 (Figure 1B center; intensity 1.7×10^8) when compared with the free carboxylate (Figure 1A center; intensity 7.1×10^6). This derivatization procedure revealed that approximately equimolar amounts of heptanone-etheno-dGuo and carboxynonanone-etheno-dGuo were formed when 13(*S*)-HPODE underwent homolytic decomposition in the presence of dGuo (Figure 1B). Therefore, DODE is an important product of 13(*S*)-HPODE decomposition. In contrast, homolytic decomposition of 15(*S*)-HPETE in the presence of dGuo produced no detectable carboxynonanone-etheno-dGuo (Figure 8). This is consistent with the proposed intermediate formation of HPODD (*12*) from 13(*S*)-HPODE and its subsequent dehydration to DODE as is observed in the dehydration of HPNE to ONE (*6*) (Scheme 1). This cannot occur with 15(*S*)-HPETE.

In summary, the finding that DODE is an important decomposition product of 13(*S*)-HPODE has implications for DNA and protein adduct formation and for lipid hydroperoxide-mediated oxidative stress. The ONE motif that is present in DODE could potentially modify arginine, lysine, cysteine, and histidine residues in proteins (*12*, *17*–*20*). The polar nature of resulting protein adducts suggests that the biological consequences could be quite different from those induced by more hydrophobic bifunctional electrophiles such as HNE and ONE. The presence of a carboxylate moiety may also make it difficult for DODE to translocate across plasma and nuclear membranes. Thus, DNA could in fact be protected against DODE-mediated DNA adduct formation. However, it is noteworthy that carboxylate-containing DNA adducts derived from leukotriene B_4 have been identified in neutrophils (*45*). Therefore, it is conceivable that there are specific transporters that facilitate the transfer of reactive carboxylate derivatives into the nucleus. In contrast, polar cytosolic glutathione (GSH)-DODE adducts may be potent inducers of oxidative stress if they are unable to translocate across the plasma membrane. It is noteworthy that inhibition of GSH-HNE adduct export from cells significantly increased cytotoxicity through potentiation of oxidative stress (*46*, *47*). Furthermore, the ONE moiety that is present in DODE has already been demonstrated to initiate apoptosis in colorectal cancer cells (*48*). The ready availability of DODE through our new synthetic method will allow a detailed exploration of its ability to induce apoptosis and also permit a rigorous characterization of its other biological activities.

Acknowledgment. We gratefully acknowledge the support of NIH Grant RO1 CA 91016.

References

(1) Laneuville, O., et al. (1995) Fatty acid substrate specificities of human prostaglandin-endoperoxide H synthase-1 and -2. *J. Biol. Chem. 270*, 19330−19336.

(2) Brash, A. R. (1999) Lipoxygenases: Occurrence, functions, catalysis, and acquisition of substrate. *J. Biol. Chem. 274*, 23679−23682.

(3) Porter, N. A., Caldwell, S. E., and Mills, K. A. (1995) Mechanisms of free radical oxidation of unsaturated lipids. *Lipids 30*, 277−290.

(4) Esterbauer, H., Schaur, R. J., and Zollner, H. (1991) Chemistry and biochemistry of 4-hydroxynonenal, malonaldehyde and related aldehydes. *Free Radical Biol. Med. 11*, 81−128.

(5) Spiteller, P., Kern, W., Reiner, J., and Spiteller, G. (2001) Aldehydic lipid peroxidation products derived from linoleic acid. *Biochim. Biophys. Acta 1531*, 188−208.

(6) Lee, S. H., Oe, T., and Blair, I. A. (2001) Vitamin C-induced decomposition of lipid hydroperoxides to endogenous genotoxins. *Science 292*, 2083−2086.

(7) Schneider, C., Tallman, K. A., Porter, N. A., and Brash, A. R. (2001) Two distinct pathways of formation of 4-hydroxynonenal. Mechanisms of nonenzymatic transformation of the 9- and 13-hydroperoxides of linoleic acid to 4-hydroxyalkenals. *J. Biol. Chem. 276*, 20831−20838.

(8) Blair, I. A. (2001) Lipid hydroperoxide-mediated DNA damage. *Exp. Gerontol*. *36*, 1473−1481.

(9) Lee, S. H., and Blair, I. A. (2001) Oxidative DNA damage and cardiovascular disease. *Trends Cardiovasc. Med. 9*, 148−155.

(10) Horkko, S., Binder, C. J., Shaw, P. X., Chang, M. K., Silverman, G., Palinski, W., and Witztum, J. (2002) Immunological responses to oxidized LDL. *Free Radical Biol. Med. 28*, 1771−1779.

(11) Liu, K., Raina, A. K., Smith, M. A., Sayre, L. M., and Perry, G. (2003) Hydroxynonenal, toxic carbonyls, and Alzheimer disease. *Mol. Aspects Med. 24*, 305−313.

(12) Uchida, K. (2003) 4-Hydroxy-2-nonenal: A product and mediator of oxidative stress. *Prog. Lipid Res. 42*, 318−343.

(13) Rindgen, D., Nakajima, M., Wehrli, S., Xu, K., and Blair, I. A. (1999) Covalent modifications to 2′-deoxyguanosine by 4-oxo-2-nonenal a novel product of lipid peroxidation. *Chem. Res. Toxicol. 12*, 1195−1204.

(14) Rindgen, D., Lee, S. H., Nakajima, M., and Blair, I. A. (2000) Formation of a substituted 1,N^6-etheno-2′-deoxyadenosine adduct by lipid hydroperoxide-mediated generation of 4-oxo-2-nonenal. *Chem. Res. Toxicol. 13*, 846−852.

(15) Lee, S. H., Rindgen, D., Bible, R. A., Hajdu, E., and Blair, I. A. (2000) Characterization of 2′-deoxyadenosine adducts derived from 4-oxo-2-nonenal, a novel product of lipid peroxidation. *Chem. Res. Toxicol. 13*, 565−574.

(16) Pollack, M., Oe, T., Lee, S. H., Silva Elipe, M. V., Arison, B. H., and Blair, I. A. (2003) Characterization of 2′-deoxycytidine adducts derived from 4-oxo-2-nonenal, a novel lipid peroxidation product. *Chem. Res. Toxicol*. *16*, 893−900.

(17) Oe, T., Lee, S. H., Silva Elipe, M. V., Arison, B. H., and Blair, I. A. (2003) A novel lipid hydroperoxide-derived modification to arginine. *Chem. Res. Toxicol. 16*, 1598−1605.

(18) Oe, T., Arora, J. S., Lee, S. H., and Blair, I. A. (2003) A novel lipid hydroperoxide derived cyclic covalent modification to histone H4. *J. Biol. Chem. 278*, 42098−43105.

(19) Liu, Z., Minkler, P. E., and Sayre, L. M. (2003) Mass spectroscopic characterization of protein modification by 4-hydroxy-2-(*E*)-nonenal and 4-oxo-2-(*E*)-nonenal. *Chem. Res. Toxicol. 16*, 901−911.

(20) Zhang, W. H., Liu, J., Xu, G., Yuan, Q., and Sayre, L. M. (2003) Model studies on protein side chain modification by 4-oxo-2-nonenal. *Chem. Res. Toxicol. 16*, 512−523.

(21) Lee, S. H., Oe, T., and Blair, I. A. (2002) 4,5-Epoxy-2(*E*)-decenal-induced formation of 1,N^6-etheno-2′-deoxyadenosine and 1,N^2-etheno-2′-deoxyguanosine adducts. *Chem. Res. Toxicol. 15*, 300−304.

(22) Akasaka, S., and Guengerich, F. P. (1999) Mutagenicity of site-specifically located 1,N^2-ethenoguanine in Chinese hamster ovary cell chromosomal DNA. *Chem. Res. Toxicol. 12*, 501−507.

(23) Levine, R. L., Yang, I.-Y., Hossain, M., Pandya, G., Grollman, A. P., and Moriya, M. (2000) Mutagenesis induced by a single 1,N^6-ethenodeoxyadenosine adduct in human cells. *Cancer Res. 60*, 4098−4104.

(24) Douki, T., Odin, F., Caillat, S., Favier, A., and Cadet, J. (2004) Predominance of the 1,N2-propano 2′-deoxyguanosine adduct among 4-hydroxy-2-nonenal-induced DNA lesions. *Free Radical Biol. Med. 37*, 62−70.

(25) Nath, R. G., Ocando, J. E., Guttenplan, J. B., and Chung, F.-L. (1998) 1,N2-propanodeoxyguanosine adducts: Potential new biomarkers of smoking-induced DNA damage in human oral tissue. *Cancer Res. 581*, 581−584.

(26) Sodum, R. S., and Chung, F.-L. (1991) Stereoselective formation of in vitro nucleic acid adducts by 2,3-epoxy-4-hydroxynonanal. *Cancer Res. 51*, 137−143.

(27) Xu, G., Liu, Y., Kansal, M. M., and Sayre, L. M. (1999) Rapid cross-linking of proteins by 4-keto aldehydes and 4-hydroxy-2-alkenals does not arise from the lysine-derived monoalkylpyrroles. *Chem. Res. Toxicol. 12*, 855−861.

(28) Salomon, R. G., Kaur, K., Podrez, E., Hoff, H. F., Krushinsky, A. V., and Sayre, L. M. (2000) HNE-derived 2-pentylpyrroles are generated during oxidation of LDL, are more prevalent in blood plasma from patients with renal disease or atherosclerosis, and are present in atherosclerotic plaques. *Chem. Res. Toxicol. 13*, 557−564.

(29) Schaur, R. J. (2003) Basic aspects of the biochemical reactivity of 4-hydroxynonenal. *Mol. Aspects Med. 24*, 149−159.

(30) Gardner, H. W., and Hamberg, M. (1993) Oxygenation of 3(Z)-nonenal to 2(E)-4-hydroxy-2-nonenal in the broad bean (Vicia faba L.). *J. Biol. Chem. 268*, 6971−6977.

(31) Gallasch, B. A. W., and Spiteller, G. (2000) Synthesis of 9,12-dioxo-10(*Z*)-dodecanoic acid, a new fatty acid metabolite derived from 9-hydroperoxy-10,12-octadecadienoic acid in lentil seed (*Lens culinaris* Medik.). *Lipids 35*, 953−960.

(32) Gardner, H. W. (1998) 9-Hydroxy-traumatin, a new metabolite of the lipoxygenase pathway. *Lipids 33*, 745−749.

(33) Noordermeer, M. A., Feussner, I., Kolbe, A., Veldink, G. A., and Vliegenthart, J. F. G. (2000) Oxygenation of (3Z)-alkenals to 4-hydroxy-(2E)-alkenals in plant extracts: a nonenzymatic process. *Biochem. Biophys. Res. Commun. 277*, 112−116.

(34) Loidl-Stahlhofen, A., Hannemann, K., and Spiteller, G. (1994) Generation of α-hydroxyaldehydic compounds in the course of lipid peroxidation. *Biochim. Biophys. Acta 1213*, 140−148.

(35) Mlakar, A., and Spiteller, G. (1994) Reinvestigation of lipid peroxidation of linolenic acid. *Biochim. Biophys. Acta 1214*, 209−220.

(36) Kawai, Y., Uchida, K., and Osawa, T. (2004) 2′-Deoxycytidine in free nucleosides and double-stranded DNA as the major target of lipid peroxidation products. *Free Radical Biol. Med. 36*, 529−541.

(37) Lee, S. H., and Blair, I. A. (2000) Characterization of 4-oxo-2-nonenal as a novel product of lipid peroxidation. *Chem. Res. Toxicol. 13*, 698−702.

(38) Lee, S. H., Williams, M. V., DuBois, R. N., and Blair, I. A. (2003) Targeted lipidomics using electron capture atmospheric pressure chemical ionization mass spectrometry. *Rapid Commun. Mass Spectrom*. *17*, 2168−2176.

(39) Deng, Y., and Salomon, R. G. (1998) Total synthesis of γ-hydroxy-α,β-unsaturated aldehydic esters of cholesterol and 2-lysophosphatidylcholine. *J. Org. Chem. 63*, 7789−7794.

(40) Sun, M., Deng, Y., Batyreva, E., Sha, W., and Salomon, R. G. (2002) Novel bioactive phospholipids: Practical total syntheses of products from the oxidation of arachidonic and linoleic esters of 2-lysophosphatidylcholine1. *J. Org. Chem. 67*, 3575−3584.

(41) Kobayashi, Y., Nakano, M., Kumar, G. B., and Kishihara, K. (1998) Efficient conditions for conversion of 2-substituted furans into 4-oxygenated 2-enoic acids and its application to synthesis of (+)-aspicilin, (+)-patulolide A, and (−)-pyrenophorin. *J. Org. Chem. 63*, 7505−7515.

(42) Batterham, T. (1982) *NMR Spectra of Simple Heterocycles*, Robert E. Krieger Publishing Company, Malabar, FL.

(43) Pretsch, E., Buhlmann, P., and Affolter, C. (2000) *Structure Determination of Organic Compounds. Tables of Spectral Data*, Springer-Verlag, Berlin.

(44) Kalinowski, H. O., Berger, S., and Braun, S. (1988) *Carbon-13 NMR Spectroscopy*, John Wiley & Sons, New York.

(45) Hankin, J. A., Jones, D. N., and Murphy, R. C. (2003) Covalent binding of leukotriene A4 to DNA and RNA. *Chem. Res. Toxicol*. *16*, 551−561.

(46) Awasthi, Y. C., Sharma, R., Cheng, J. Z., Yang, Y., Sharma, A., Sighal, S. S., and Awashti, S. (2003) Role of 4-hydroxynonenal in stress-mediated apoptosis signaling. *Mol. Aspects Med. 24*, 219−230.

(47) Awasthi, Y. C., Yang, Y., Tiwari, N. K., Patrick, B., Sharma, A., Li, J., and Awashti, S. (2004) Regulation of 4-hydroxynonenal-mediated signaling by glutathione S-transferases. *Free Radical Biol. Med. 37*, 607−619.

(48) West, J. D., et al. (2004) Induction of apoptosis in colorectal carcinoma cells treated with 4-hydroxy-2-nonenal and structurally related aldehydic products of lipid peroxidation. *Chem. Res. Toxicol. 17*, 453−462.

TX049716O